ALBEDO AND TRANSMITTANCE OF CUMULUS CLOUDS

G.A. Titov

Institute of Atmospheric Optics,
Siberian Branch of the Russian Academy of Sciences, Tomsk
Received May 20, 1995

A 3D model of solar radiative transfer in statistically inhomogeneous cumulus clouds is considered. It is shown that the 2D albedo and transmittance fields are highly variable in horizontal direction. For an individual pixel the sum of the albedo and transmittance may substantially differ from unity. The Independent Pixel Approximation, disregarding the horizontal radiative transfer, unsatisfactorily describes the radiative effects in cumulus clouds.

1. INTRODUCTION

Current radiation codes of general circulation models (GCM's) are still mostly based on plane-parallel model, which unsatisfactorily describes the radiative effects of inhomogeneous stratus and cumulus clouds because their optical characteristics are
highly variable in vertical and horizontal directions. Updated GCM parameterization of interaction of radiation with cumulus clouds calls for both novel observational data and more realistic radiative transfer models. In this paper, we present a 3D model of radiative transfer used to study the relationship between the spatial distribution of cumulus clouds and fluxes (albedo and transmittance) of visible solar radiation.

In the visible, the scattering by water droplets can be assumed conservative (the single scattering albedo is unity), so that mean albedo $\bar{R}$ and transmittance $\bar{Q}$ are related by the formula $\bar{R} + \bar{Q} = 1$ expressing the radiative energy balance. Let clouds occupy a certain spatial domain in the form of parallelepiped with thickness ΔH and square base of side length Xl. In the horizontal plane we divide the domain into cells (pixels) of equal size Δl, and for each of these cells calculate the albedo $R_{i,j}$ and transmittance $Q_{i,j}$, $i, j = 1, \ldots, nx$, where $nx = Xl/\Delta l$ is the number of cells along each of the coordinate axes OX and OY. The number of cells is nx^2.

When the domain is a part of a plane-parallel cloud, then on account of the homogeneous boundary conditions, the equality $Q_{i,j} + R_{i,j} = 1$, $i, j = 1, \ldots, nx$, holds true for each cell. Will the same equality hold true in the *cumulus* cloud case? What consequences will have the *horizontal inhomogeneity* of cumulus clouds on the spatial distribution of uniform incident solar flux? The mathematical simulation results we present below answer some of these questions, as well as make it possible to obtain the probability densities and energy distribution of albedo and transmittance in *statistically inhomogeneous* cumulus clouds.

2. MODEL OF CUMULUS CLOUDS AND METHOD OF SOLUTION

The stochastic geometry of cumulus clouds is yet poorly understood. To avoid lengthy computations, we use a simple model of cumulus clouds simulated with the help of the Poisson point process in space. Cumulus clouds are approximated by inverted truncated paraboloids of rotation with height H being equal to their diameter D. The latter has the exponential distribution function $f(D) \sim \exp(-\alpha D)$, $D_{\min} \le D \le D_{\max}$. Optical parameters (extinction coefficient, single scattering albedo, and scattering phase function) are assumed constant within the cloud. The radiative effects of the atmospheric aerosol and the underlying surface are neglected for simplicity.

A computer realization of cloud field for pixel horizontal size $\Delta l = 0.1$ km, $nx = 64$ ($nx^2 = 4096$ and $Xl = 6.4$ km), $\alpha = 2$, $D_{\min} = 0.03$ km, $D_{\max} = 1.2$ km, cloud fraction $N = 0.5$, and the extinction coefficient $\sigma = 20$ km^{-1} is displayed in Fig. 1*a*. If a cell belongs to a group of (two or more) clouds, its optical thickness is calculated for the largest cloud in the group.

The 3-D equation of transfer was solved with periodic boundary conditions assuming that the entire layer $0 \le z \le \Delta H$ is filled by the given cloud field realization. Radiant fluxes were computed by the Monte Carlo (MC) method for one or more hundred million trajectories, which ensured relative error no more than 2%. The cell averaged transmittance was determined at the lower cloud boundary (plane $z = 0$) and the albedo - at the upper (plane $z = \Delta H$) cloud boundary. Details of the cumulus cloud model and the MC algorithms can be found in Refs. 1 and 2. All calculations below employ Henyey-Greenstein scattering phase function with an asymmetry parameter of 0.843 (typical of wavelengths 0.3–3.0 μm). The solar azimuth angle, measured from the OX axis, was zero.

0235-6880/96/01 1-06 $02.00

3. THE 2-D ALBEDO AND TRANSMITTANCE FIELDS

Multiple scattering plays a dominant role in the formation of radiative field in clouds; therefore, the albedo R and diffuse transmittance Q_s reach large values even in cloudless cells (Figs. 1*b* and *d*). In the given cloud field realization, clouds vary in thickness from 0.033 to 1.174 km. Radiative field, reflected by a single cloud, spreads in space and overlaps with the fields from the other clouds before reaching the plane $z = \Delta H$ of albedo definition. Owing to the spread and overlap effects, the albedo is essentially smoothed out in the horizontal plane, so that many details are masked, thereby complicating the visual reconstruction of the real pattern of cloud spatial distribution from the known albedo values (Figs. 1*a* and *b*). Tops of the densest clouds are distinctly observed since for them the effects above are not so strong. The albedo varies from 0.24 to 0.65.

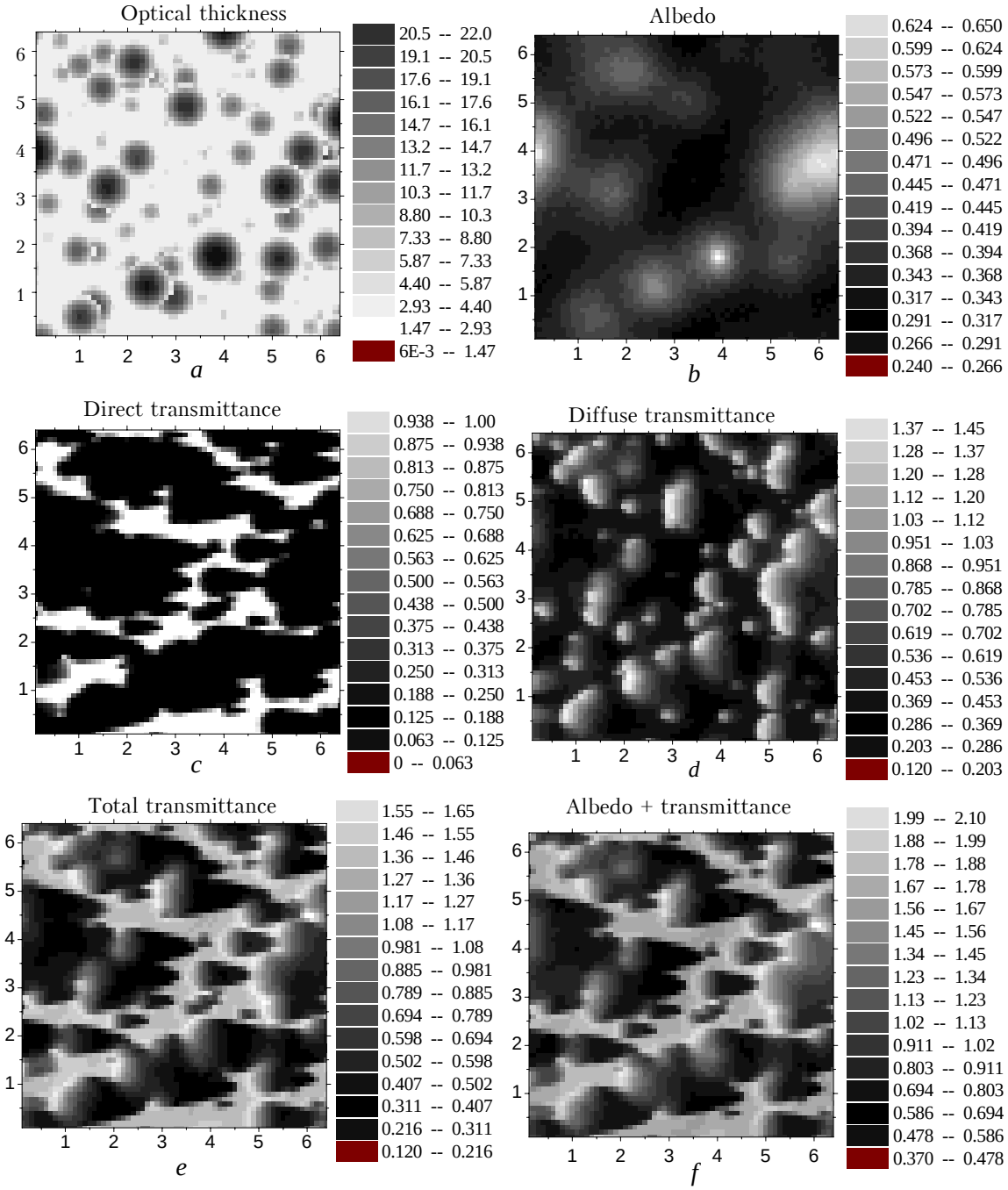

FIG. 1. The 2-D fields of optical depth (a), albedo (b), transmittance of direct (c), diffuse (d), and total radiation (e), and albedo plus transmittance (f) for the cloud fraction $N = 0.5$, *pixel horizontal size of* 0.1 km, *extinction coefficient* $\sigma = 20$ km^{-1}, *and solar zenith angle* $\xi_{\oplus} = 60°$.

The transmittance S of direct radiation passing through gaps between clouds is unity (the direction toward the sun is cloud-free), and at oblique solar zenith angles the cloud shadows are clearly seen (Fig. 1*c*). Optically thin regions, localized near the cloud bottom and sunlit, transmit much of the radiation without scatter, thereby slightly smearing shadow boundaries.

The diffuse transmittance Q_s is maximum for those cells that have small (roughly 2–3) optical thickness and are not screened by surrounding clouds, i.e., the incident solar radiation reaches them without interaction with clouds (Fig. 1*d*). Interestingly Q_s for such cells may be much greater than unity, owing to the radiation being incident on the neighboring optically thicker cells and after multiple scattering, sliding into these optically thinner cells and passing through them. Certainly, there exist cells with small (0.1–0.2) Q_s values, either far apart from the clouds or within the shadow zones of densest clouds. As a result, the diffuse transmittance may vary by more than an order of magnitude (from 0.12 to 1.45).

The transmittance of total radiation, $Q = S + Q_s$, is displayed in Fig. 1*e*. The 2D transmittance field was calculated in the plane $z = 0$ of the lower cloud boundary. This circumstance as well as strong elongation of the scattering phase function of cloud droplets and the direct radiation contribution lead to the fact that the transmittance field of total radiation is much less smoothed in space than the albedo field. A small fraction of the incident solar radiation may reach pixels located within shadows from densest cumulus clouds. For this reason, smallest Q values occur in such cells independent of their optical thickness. For cells located in cloud gaps $S = 1$, and due to excess diffuse radiation contribution, the inequality $Q > 1$ always holds true. Clearly, this inequality will also hold for those cells where $Q_s > 1$. The $Q > 1$ values have long been obtained in field measurements[3]; however, no such theoretical estimates of Q were previously reported, as far as we know.

The simulation results indicate that the albedo and transmittance of cumulus have large horizontal gradients. As a result, the radiative energy balance is obeyed on average, for the entire spatial domain under consideration, but in each cell the sum $Q_{i,j} + R_{i,j}$, $i,j = 1, \ldots, nx$, may substantially differ from unity, ranging from 0.37 to 2.10 (Fig. 1*f*).

The effect of local deviation of the radiative energy balance from unity seems highly important as it clearly demonstrates that some familiar patterns of transfer determined for plane-parallel cloud model may be violated for the radiative characteristics and brightness fields of inhomogeneous cloud system. Neglect of this fact may lead to incorrect physical interpretation of field measurements for real clouds. That way, from the albedo and transmittance measurements for a small number of pixels, erroneous conclusion can be drawn that a strong absorber (amplifier) is present in clouds. The horizontal inhomogeneity of radiant fluxes in cumulus can appreciably affect such atmospheric processes as underlying surface heating, cloud dynamics, and photochemical reactions, among many others.

4. ALBEDO AND TRANSMITTANCE STATISTICS

Minimum and maximum values, mean and variance of optical depth, albedo, various components of transmittance, and albedo plus transmittance are tabulated in Table I. Also tabulated are the probabilities $P\{Q > 1\}$ and $P\{Q + R > 1\}$ that Q and $Q + R$ values exceed unity. Minimum τ and S values are zero, while $S_{\max} = 1$. The theoretical estimates of $P\{Q > 1\}$ agree well with shipboard measurements made in the tropics of the Pacific Ocean (the underlying surface albedo is close to zero): for a cumulus cloud fraction of 0.6 to 0.8 this probability is approximately equal to 0.16 (Ref. 4). As seen, there is a considerable deviation of the radiative energy balance from unity for all cloud fractions. Values $Q > 1$ and $Q + R > 1$ are frequent for small cloud fractions, with *vice versa* for large N. In accordance with aforesaid, the variance of albedo is much less than the variance of transmittance.

TABLE I. The statistical characteristics of optical depth, albedo, and transmittance of visible solar radiation calculated for indicated cloud fractions with $\sigma = 20$ km^{-1} *and* $\xi_\oplus = 60°$.

Characteristics		Cloud fraction			
		0.1	0.3	0.5	0.7
τ	max	22.78	22.82	23.25	23.76
	mean	0.73	2.29	4.03	6.70
	variance	8.64	20.70	30.69	38.69
S	mean	0.83	0.53	0.25	0.05
	variance	0.1253	0.2166	0.1494	0.0294
Q_s	min	0.02	0.05	0.12	0.15
	max	1.21	1.37	1.45	1.58
	mean	0.11	0.28	0.42	0.45
	variance	0.0355	0.0696	0.0758	0.0557
Q	min	0.03	0.08	0.12	0.15
	max	1.39	1.51	1.65	1.82
	mean	0.94	0.81	0.67	0.50
	variance	0.0834	0.1720	0.1839	0.0925
	$P\{Q > 1\}$	0.80	0.55	0.30	0.10
R	min	0.03	0.10	0.24	0.34
	max	0.444	0.56	0.65	0.80
	mean	0.068	0.19	0.33	0.50
	variance	0.0012	0.0025	0.0039	0.0060
$R+Q$	min	0.08	0.20	0.38	0.54
	max	1.53	1.77	2.10	2.38
	variance	0.0790	0.1632	0.1781	0.1024
	$P\{Q+R>1\}$	0.84	0.59	0.40	0.32

The probability densities of albedo $f(R)$ and transmittance of total radiation $f(Q)$ are shown in Fig. 2. As N increases, the mode of $f(R)$ shifts toward larger R values, the variance increases, and the

distribution gets more symmetric. For small and intermediate N values, the probability density of transmittance has two distinct maxima, a physically clear result. Bimodal $f(Q)$ was also obtained after processing of experimental data in Refs. 3 and 4.

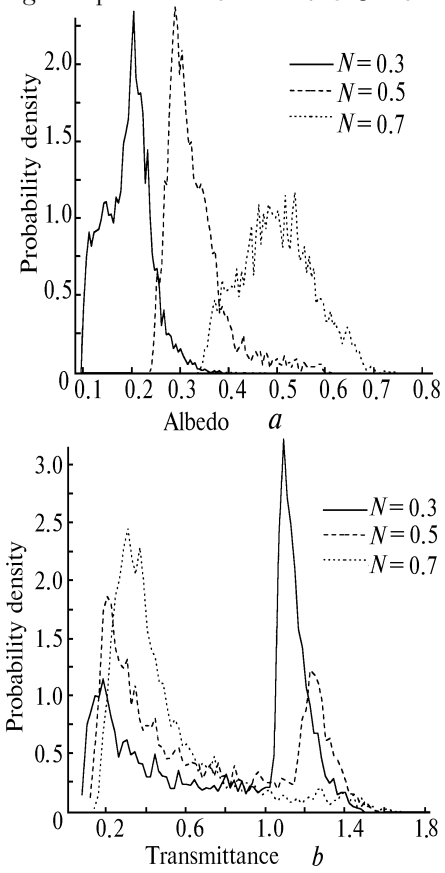

FIG. 2. Probability densities of albedo (a) and transmittance (b) of solar radiation at the cloud bottom level with $\xi_{\oplus} = 60°$, $\sigma = 20$ km^{-1}, *and indicated cloud fractions.*

Figure 3 shows the spectral power density E of optical depth, albedo, and transmittance versus bin number $k = \omega_k \cdot Xl$ on log-log scale, where ω_k is the spatial frequency. The effects of multiple scattering, spread, and overlap smooth much better the field of reflected solar radiation than that of transmitted radiation; so $E(R)$ is much narrower and differs stronger from $E(\tau)$ than $E(Q)$ does.

The statistical characteristics of transmittance discussed above were obtained for the altitude of the cloud bottom. In practice, the transmittance of solar radiation is usually measured by a device located at the underlying surface (US). Because the spread and overlap effects of cloud radiation fields are altitude-dependent, so do the probability densities of transmittance $f(Q)$ (Fig. 4*a*). Peaks of $f(Q)$ on the surface occur at larger Q, while at $N = 0.7$ the distribution becomes narrower. For small N the probability density $f(R+Q)$ is bimodal (Fig. 4*b*). The calculation results indicate that $f(R+Q)$ depends on the altitude of transmittance measurement only weakly.

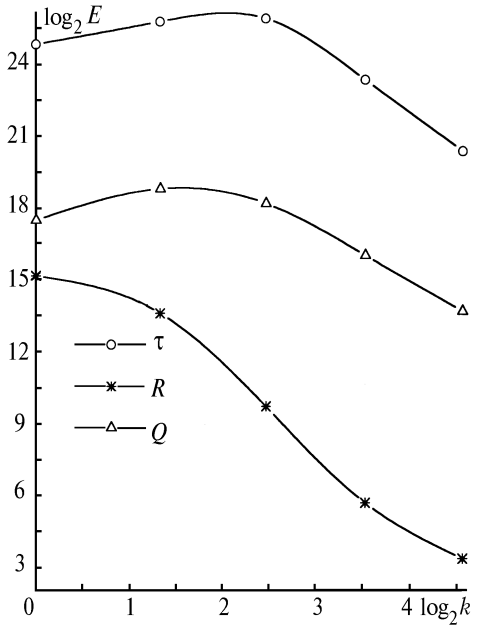

FIG. 3. Spectral power density E of optical depth, albedo and transmittance versus bin number k with $\xi_{\oplus} = 60°$, $N = 0.5$, *and* $\sigma = 20$ km^{-1}.

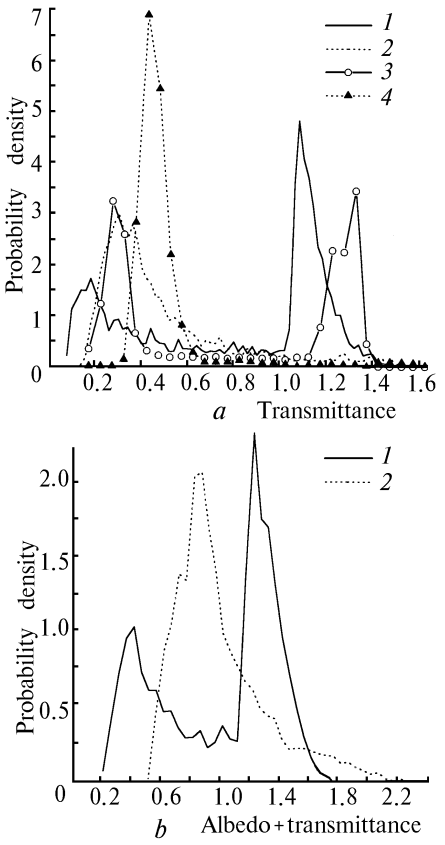

FIG. 4. The probability densities of transmittance of total radiation (a) and the sum $R + Q$ *(b) with* $\xi_{\oplus} = 60°$, $\sigma = 20$ km^{-1}, *and* $N = 0.3$ *(1, 3) and* 0.7 *(2, 4): 1, 2) at the cloud bottom and 3, 4) at the underlying surface. The cloud base altitude is* 1 km.

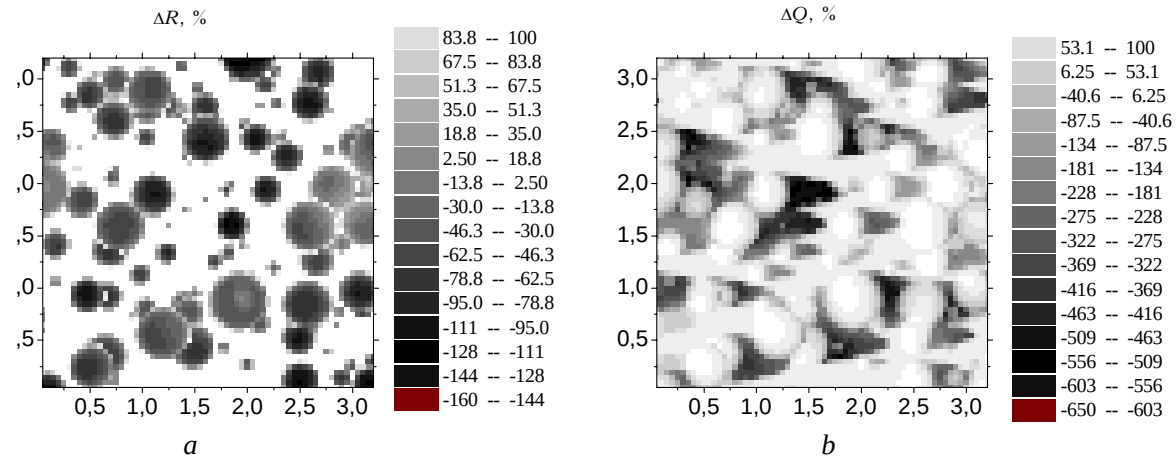

FIG. 5. The 2D fields ΔR *and* ΔQ *for cloud fraction* $N = 0.5$, *pixel horizontal size of* 0.1 km, *extinction coefficient* $\sigma = 20\ \text{km}^{-1}$, *and solar zenith angle* $\xi_\oplus = 60°$.

5. INDEPENDENT PIXEL APPROXIMATION (IPA)

This approximation neglects horizontal radiative transfer and uses the plane-parallel model for each pixel (cell).[5,6] In other words, radiative properties of each cloud pixel depend only on its vertical optical thickness, and do not depend on the optical thickness of neighboring pixels. In the case of plane-parallel stratocumulus clouds with nonuniform distribution of optical depth, the IPA has reasonable accuracy given that horizontal size of a pixel exceeds its thickness and is much larger than the photon mean free path in clouds. Otherwise, the estimated mean albedo is biased by 10–20%. In the IPA, the albedo R_{IPA} and transmittance Q_{IPA} can be calculated for each pixel using formulas that for conservative scattering have the form[7]

$$R_{\text{IPA}}(\tau;\ \xi_\oplus,\ g)=1-Q_{\text{IPA}}(\tau;\ \xi_\oplus,\ g),$$

$$Q_{\text{IPA}}(\tau;\ \xi_\oplus,\ g) = \frac{\delta(\xi_\oplus) + [1 - \delta(\xi_\oplus)]\exp[-\tau / |\, a(\xi_\oplus)|\,]}{1 + \gamma(g)\tau}, \qquad (1)$$

where τ is the pixel optical thickness, $\xi_\oplus$ is the solar zenith angle, and g is the asymmetry parameter. Below we use the following values of the functions $\delta(\xi_\oplus)$, $a(\xi_\oplus)$, and $\gamma(g)$: $\delta(60°)=0.8$, $a(60°)=0.8$, and $\gamma(0.843)=0.11$.

Much larger albedo biases are expected for cumulus clouds, whose geometry is radically different from plane-parallel, because the effects associated with their stochastic geometry (shading and multiple scattering between clouds) influence profoundly the solar radiative transfer. From Eq. (1) it follows that the 2D fields R_{IPA} and Q_{IPA} follow the distribution of optical thickness (Fig. 1*a*), and hence visually they are very dissimilar to their MC counterparts, R and Q fields (Figs. 1*b* and *e*). In particular, R_{IPA} and Q_{IPA} have zero values in the pixels located in gaps between clouds, Q_{IPA} never exceeds unity, and the radiative energy balance $R + Q = 1$ holds true for each pixel. Obviously the IPA fails to describe the spread and overlap effects for radiation fields of individual clouds.

The MC versus IPA comparison in cumulus is performed by calculating

$$\Delta R = \frac{R + R_{\text{IPA}}}{R}\,100\%, \quad \Delta Q = \frac{Q + Q_{\text{IPA}}}{Q}\,100\%,$$

where Q values are calculated at the cloud bottom level. The IPA underestimates the albedo for pixels located in gaps between clouds, with *vice versa* for the other pixels (Fig. 5*a*). The IPA-calculated mean and variance of the albedo are 0.25 and 0.0807, respectively. Compared with the MC values above, the IPA gives the mean albedo being about a factor of 1.5 lower and the variance being 20 times higher. This suggests that the radiative interaction of pixels and the effects of stochastic geometry effectively smooth out the reflected field of solar radiation.

The transmittance Q exceeds Q_{IPA} in the pixels located in the optically thin regions of cloud base or in cloud gaps, both directly sunlit, i.e., not shaded by clouds (Fig. 5*b*). As expected, $|\Delta Q|$ assumes maximum values in the pixels located in cloud gaps and shaded by clouds. Values of Q may be far in excess of unity, so that the variance of Q is twice that of Q_{IPA}.

Summarizing, the results above clearly demonstrate that IPA *unsatisfactorily* describes the radiation effects of cumulus clouds.

Undoubtedly, allowance for interaction of solar radiation with the atmospheric aerosols and the underlying surface as well as the use of updated and more sophisticated cumulus cloud models will somewhat alter the quantitative estimates of statistical characteristics of albedo, transmittance, and their sum; however, this by no means degrades the reliability of the qualitative results concerning the influence of cloud horizontal inhomogeneity on the 2D fields of visible solar radiation fluxes, as they have clear physical foundation.

Presently the scarcity of experimental data on stochastic cumulus clouds presents a major obstacle to developing the 3-D radiative transfer models for cumulus clouds. With the availability of more data it will be possible to improve the existing models and, if necessary, to develop novel, more realistic ones for treating the solar and infrared radiative transfer in cumulus clouds.

ACKNOWLEDGMENTS

This work was supported in part by DOE ARM Program Contract No. 350114-A-Q1, International Science Foundation and Russian Government Grant No. JI7100, and Russian Foundation for Fundamental Research Grant No. 95-05-14162.

REFERENCES

1. G.A. Titov, J. Atm. Sci. **47**, No. 1, 24–38 (1990).
2. V.E. Zuev and G.A. Titov, J. Atm. Sci. **51**, No. 2, 176–190 (1995).
3. R.G. Timanovskaya and E.M. Feigel'son, Meteor. Gidrol., No. 11, 44–51 (1970).
4. R.G. Timanovskaya and S.D. Timanovskii, Izv. Ros. Akad. Nauk, Ser. Fiz. Atmos. Okeana **30**, No. 2, 278–286 (1994).
5. R.F. Cahalan, in: *Advances in Remote Sensing Retrieval Methods*, Deepak Pub. (1989), pp. 371–388.
6. R.F. Cahalan, W. Ridgway, W.J. Wiscombe, T.L. Bell, and J.B. Snider, J. Atmos. Sci. **51**, 2434–2455 (1994).
7. M.D. King and Harshvardhan, J. Atmos. Sci. **43**, 784–801 (1986).